Structure and Conformation of DAB Dendrimers in Solution via Multidimensional NMR Techniques

Minghui Chai, Yanhui Niu, Wiley J. Youngs, and Peter L. Rinaldi*

Contribution from the Department of Chemistry, Knight Chemical Laboratory, The University of Akron, Akron, Ohio 44325-3601

Received July 31, 2000. Revised Manuscript Received March 5, 2001

Abstract: NOESY−HSQC 3D-NMR and NOESY 2D-NMR techniques have been used on a 750 MHz spectrometer to study the chain conformations of different generation DAB dendrimers (poly[propylene imine] dendrimers) in chloroform and benzene solutions. The high-field multidimensional NMR techniques provided the chemical shift dispersion needed to resolve all of the unique resonances in the dendrimers. By studying the NOE interactions among dendritic chain protons, information about through space interactions between protons on different parts of the dendrimer chain is obtained, which is directly related to the conformation of the dendrimer. These experiments also give further proof of the chemical shift assignments obtained from the HMQC-TOCSY 2D and 3D NMR experiments. The concentration effects on chemical shifts have also been observed, revealing information about the interactions between solvent and different parts of dendrimer molecules. These studies clearly show for DAB dendrimers, that folded chain conformations can occur in nonpolar solvents such as benzene and extended chain conformations are predominant in polar solvents such as chloroform.

Introduction

Dendrimers, which are highly symmetrical cascade polymers, have drawn significant attention since the first successful synthesis was reported in 1985.[1] This is partly a result of their unique physical and chemical properties[2] such as low intrinsic viscosity, high solubility, high miscibility, and high reactivity. The coexisting features, extensive branching and high surface functionality, have distinguished dendrimers from the classic linear and cross-linked polymers. Various novel dendrimers have been designed and synthesized.[3]

The most popularly studied and commercially available dendrimers, PAMAM (poly(amidoamine)) and DAB (poly(propylene imine)) dendrimers,[1,4] are made by a divergent strategy. DAB dendrimers (Scheme 1) were first synthesized by de Brabander-van den Berg and Meijer in 1993.[5] Coincidentally similar dendrimers, poly(trimethylene imines), were made by Wörner and Mülhaupt.[6] Since then, many studies have been reported on DAB dendrimers and their derivatives: such as molecular recognition, physical encapsulation, and self-assembly. Meijer's dendritic box[7] was used to demonstrate the feasibility of temporary and selective encapsulation of small molecules within the dendritic voids. This shows the great potential for DAB dendrimers to be used for biomedical applications such as drug delivery systems. Unlike the PAMAM system, the DAB system has only aliphatic spacers separating trifurcate sites, and can be expected to be more biocompatible. Scherrenberg et al.[8] studied the molecular characteristics of DAB dendrimers via small-angle neutron scattering (SANS), viscometry, and molecular dynamics simulations. On the basis of their simulations, they predicted the amine chain ends on the surface should exhibit a substantial degree of backfolding.

The conformations of dendrimers in the solid state and in solution are still uncertain. Controversial predictions of the shape of dendritic molecules have been made based on theoretical modeling and computer simulations. de Gennes and Hervet[9] proposed a model that has a density minimum at the center of the dendrimer and a density maximum on the surface, based on a self-consistent mean-field analysis. Maciejewski suggested that an outer barrier, or shell, can be formed in large dendritic molecules, which limits access to the interior of the molecule.[10]

* Address correspondence to this author. Telephone: 330-972-5990. Fax: 330-972-5256. E-mail: PeterRinaldi@uakron.edu.

(1) (a) Tomalia, D. A.; Baker, H.; Dewald, J.; Hall, M.; Kallos, G.; Martin, S.; Roeck, J.; Ryder, J.; Smith, P. *Polym. J. (Tokyo)* **1985**, *17*, 117. (b) Tomalia, D. A.; Baker, H.; Dewald, J.; Hall, M.; Kallos, G.; Martin, S.; Roeck, J.; Ryder, J.; Smith, P. *Macromolecules* **1986**, *19*, 2466.

(2) (a) Fréchet, J. M. J.; Hawker, C. J.; Gitsov, I.; Leon, J. W. *J. Macromol. Sci. Pure* **1996**, *A33*, 1399. (b) Fréchet, J. M. J. *Science* **1994**, *263*, 1710. (c) Wooley, K. L.; Hawker, C. J.; Lee, R.; Fréchet, J. M. J. *Polym. J.* **1994**, *26*, 187. (d) Gitsov, I.; Wooley, K. L.; Hawker, C. J.; Ivancva, P. T.; Fréchet, J. M. J. *Macromolecules* **1993**, *26*, 5621. (e) Tomalia, D. A.; Dupont-Durst, H. *Top. Curr. Chem.* **1993**, *165*, 193. (f) Hawker, C. J.; Wooley, K. L.; Fréchet, J. M. J. *J. Chem. Soc., Perkin Trans. 1* **1993**, *1993*, 1287. (g) Mourey, T. H.; Turner, S. R.; Rubinstein, M.; Fréchet, J. M. J.; Hawker, C. J.; Wooley, K. L. *Macromolecules* **1992**, *25*, 2401.

(3) See reviews on dendrimers: (a) Majoral, J.-P.; Caminade, A.-M. *Chem. Rev.* **1999**, *99*, 845−880. (b) Vögtle, F. *Top. Curr. Chem.* **1998**, *197*. (c) Newkome, G. R.; Moorefield, C. N.; Vögtle, F. *Dendritic Molecules*; VCH: Weinheim, 1996. (d) Zeng, F.; Zimmerman, S. C. *Chem. Rev.* **1997**, *97*, 1681. (e) Tomalia, D. A.; Naylor, A.; Goddard, W. A. *Angew. Chem., Int. Ed. Engl.* **1990**, *29*, 138.

(4) Bosman, A. W.; Janssen, H. M.; Meijer, E. W. *Chem. Rev.*, **1999**, *99*, 1665.

(5) de Brabander-van den Berg, E. M. M.; Meijer, E. W. *Angew. Chem., Int. Ed. Engl.* **1993**, *32*, 1308.

(6) Wörner, C.; Mülhaupt, R. *Angew. Chem., Int. Ed. Engl.* **1993**, *32*, 1306.

(7) Jansen, J. F. G. A.; de Brabander-van den Berg, E. M. M.; Meijer, E. W. *Science* **1994**, *266* (18), 1226.

(8) Scherrenberg, R.; Coussens, B.; van Vliet, P.; Edouard, G.; Brackman, J.; de Brabaner, E. *Macromolecules* **1998**, *31*, 456.

(9) de Gennes, P. G.; Hervet, H. J. *Phys. Lett. Paris* **1983**, *44*, 351.

10.1021/ja002824m CCC: $20.00
Published on Web 05/01/2001

Scheme 1. Structure of DAB Dendrimers

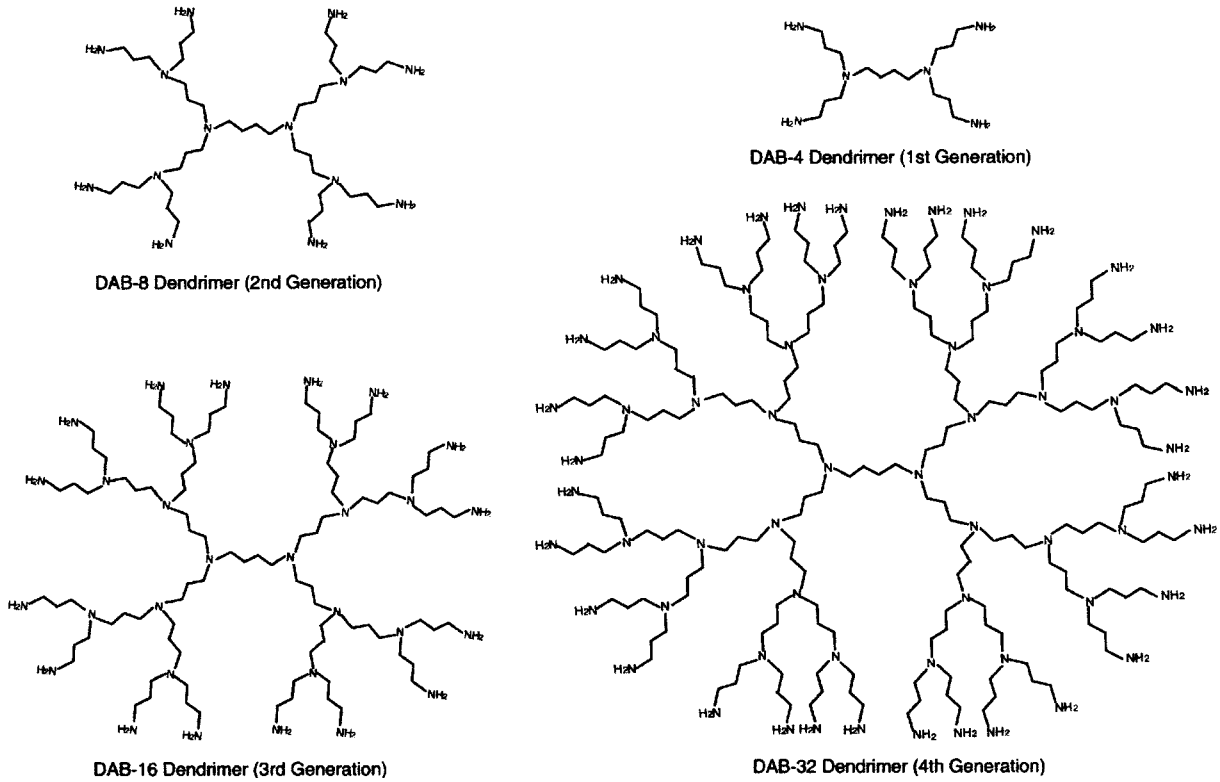

This can be considered as an extreme case of the surficial dense-packing of dendrimers in de Gennes's model.

Naylor et al.[11] used computer-assisted molecular modeling to infer that as the size increases, the dendrimer's shape progresses from an open structure to a closed spheroid with well-developed cavities and a dense surface. However, Lescanec and Muthukumar[12] have developed a simplified kinetic model by using computer simulation of dendritic growth. Their model suggests the maximum density is between the assumed dense core and the periphery of the dendrimer, because of the inward-folding of the chain ends.

Mansfield and Klushin[13] used Monte Carlo simulations on a set of diamond-lattice model dendrimers, and found that terminal groups (chain ends) are dispersed throughout the dendrimer and that a density maximum exists between the central core and the periphery. Using the same method, Welch and Muthukumar reported that a reversible transition between a "dense core" and a "dense shell" structure can be induced in dendritic polyelectrolytes by varying the ionic strength of the solvent.[14] Molecular dynamics simulations of dendrimers that incorporate solvent effects have been performed by Murat and Grest.[15] Their model predicts significant backfolding of the chain ends and a high-density area located near the core for all quality solvents (good, θ, and poor). Their model also predicts an overall increase in dendrimer density with decreasing solvent quality.

Wooley et al.[16] obtained information about dendrimer packing and estimated density in the solid state for a fifth generation benzyl ether dendrimer, based on the location of the chain ends and the range of the interpenetration as determined by rotational-echo double-resonance (REDOR) solid-state NMR experiments. They used this information together with molecular dynamics simulations to infer the conformation of the dendrimer in the solid state. They also found that density decreases near the periphery of dendrimers in the solid state because of the inward-folding of chain ends. However, some of the properties of well-known dendrimers can be explained by their globular shapes with the chain ends accessible to the surface.[2]

Recently, Topp et al.[17] described studies of DAB size changes in concentrated solution by SANS. In their work, dendrimers in dilute solutions behave as a dispersion of soft spheres with relatively uniform size. At lower concentrations, the size of the dendrimer is not strongly affected by the dendrimer's concentrations, while at certain higher concentrations, the size of dendrimer decreases as its number density increases. They speculated that the dendrimers would deform from their spherical shape and fill the voids between the spheres much like "grapes" shrinking and deforming to become "raisins". No significant interpenetration between the segments of different dendrimers were observed in their study. They used deuterated solvent CD_3OH instead of CD_3OD to prevent exchange of deuterium with the hydrogen of the terminal amine. For polar solvents such as D_2O and CD_3OH, strong hydrogen bonds can form with the amine groups of DAB; this might promote solvent penetration into the dendrimer. But for a nonpolar solvent such as benzene, the solvent molecules are less likely to penetrate into the core of the dendrimer. The information about the interior and core of the dendrimer obtained from SANS is based on detection of the deuterium in solvent molecules which have penetrated into the dendrimer. Thus the results from SANS cannot directly reflect the intrinsic conformation of the dendritic chain.

(10) Maciejewski, M. J. *Macromol. Sci. Chem.* **1982**, *A17* (4), 689.
(11) Naylor, A. M.; Goddard, W. A., III; Kiefer, G. E.; Tomalia, D. A. *J. Am. Chem. Soc.* **1989**, *111*, 2339.
(12) Lescanec, R. L.; Muthukumar, M. *Macromolecules* **1990**, *23*, 2280.
(13) Mansfield, M. L.; Klushin, L. I. *Macromolecules* **1993**, *26*, 4262.
(14) Welch, P.; Muthukumar, M. *Macromolecules* **1998**, *31*, 5892.
(15) Murat, M.; Grest, G. S. *Macromolecules* **1996**, *29*, 1278.
(16) Wooley, K. L.; Klug, C. A.; Tasaki, K.; Schaefer, J. *J. Am. Chem. Soc.* **1997**, *119*, 53.
(17) Topp, A.; Bauer, B. J.; Pross, T. J.; Scherrenberg, R.; Amis, E. J. *Macromolecules* **1999**, *32*, 8923.

Bosman et al.[18] reported the intramolecular hydrogen bonding of NH protons to nearby polar groups in a modified DAB type dendrimer system. Their results were confirmed by spectroscopic evidence from solutions of dendrimers of all generations studied. The results of their study showed that the density profiles in dendrimers, localization of end groups, and related issues depend on the structure of the dendrimer and that in performing theoretical modeling one must also consider secondary interactions such as hydrogen bonding.

The variety of contradictory conclusions from both theoretical predictions and experimental measurements indicates that more systematic experimental investigations of molecules with dendritic topology need to be done. More effective methods to study dendrimers are needed to fully understand their structures, and to guide the design and synthesis of structures for particular uses.

Utilization of NMR in biochemistry has demonstrated that it is a very powerful method. NMR surely can play an important role; in dendrimer chemistry, however, it has not been the preferred method for studying dendrimers, despite the wealth of information available from the many measurable NMR parameters. This is largely a result of the limited ability to resolve the resonances from the many unique, but very similar groups in these molecules. To date, 1D NMR has been extensively used as a routine method for characterization of dendrimers. Dynamic NMR has been used to investigate the host−guest interactions in PAMAM dendrimer systems. Both ^{2}H and ^{13}C NMR relaxation times have also been studied for these types of dendrimers by Meltzer et al.[19] These studies have shown a decrease in the spin−lattice relaxation times (T_1) of both carbon and deuterium nuclei as the number of chain termini increases. This indicates that the chain terminus has faster motion than the interior sites and that chain motion decreases as the molecular size increases. Recently, Malyarenko et al. studied ^{2}H quadrupolar echo line shapes[20] and relaxation[21] of various PAMAM generations in the solid state to learn about hydrogen bonding and molecular motion in these dendrimers. On the basis of the results, they were able to infer the degree of back-folding and interpenetration of the ends of the dendrimer arms as a function of generation length and counterion. Lambert and co-workers have used the 2D $^{29}Si-^{29}Si$ INADEQUATE experiment to confirm the structure of the first generation dendritic polysilane.[22]

Recently, three-dimensional (3D) $^{1}H/^{13}C/^{29}Si$ triple resonance NMR has been applied to fully characterize the structures of carbosilane dendrimers.[23] Although enormous spectral dispersion is provided, this 3D $^{1}H/^{13}C/X$ NMR technique cannot be effectively implemented with unenriched DAB, where $X = {}^{15}N$, because of ^{15}N's low natural abundance (0.3%). In a recent communication,[24] 3D HMQC-TOCSY[25] NMR experiments were used to characterize DAB dendrimers. This experiment provides better sensitivity (^{1}H detection) and high resolution (dispersion of resonances into three dimensions) for structural studies of dendrimers. A plane at the shift of each ^{13}C resonance will contain a peak on the diagonal at the shift of the ^{1}H bound to that ^{13}C, and off-diagonal peaks at the shifts of all the ^{1}H atoms which are a part of the same spin system. This experiment provides a powerful way to resolve and observe the resonances from atoms within each generation of the dendritic structure. In this paper, 2D-NOESY[26] and 3D-NOESY-HSQC[27] experiments have been used to study DAB dendrimers in chloroform and benzene solvents. The NOESY interactions among different protons provide information regarding their spatial locations relative to various parts of the dendritic chain. Therefore, information about the dominant conformation of the dendritic chains in solutions can be inferred. Solvent−dendrimer NOE interactions also provide information about the interactions between the dendrimer and solvent molecules in this study.

Table 1. Concentrations of DAB-16 in Different Solvents

solvent	concentration
C_6D_6:C_6H_6 (1:3)	0.40 M (500 mg/0.75 mL)
0.12 M (150 mg/0.75 mL)	
$CDCl_3$:$CHCl_3$ (1:4)	0.40 M (500 mg/0.75 mL)
0.12 M (150 mg/0.75 mL)	
C_6D_6:C_6H_6 (3:1)	0.12 M (150 mg/0.75 mL)
$CDCl_3$	0.16M (150 mg/0.75 mL)

Experimental Section

Chemicals and Sample Preparation. $CHCl_3$ and C_6H_6 solvents and all generation DAB dendrimers were obtained from Aldrich Chemical Co. Deuterated solvents $CDCl_3$ and C_6D_6 were purchased from Cambridge Isotope Laboratory (Andover, MA). Chloroform and deuterated chloroform were dried over phosphorus pentoxide and distilled before use. Benzene and deuterated benzene were dried over molecular sieve and distilled before use. All poly(propylene imine) dendrimers were pumped before use. The preparation of samples was performed in the glovebox under argon. All solutions were degassed by several freeze−pump−thaw cycles in 5 mm NMR tubes before sealing. Table 1 summarizes the samples prepared.

Hardware for NMR Measurement and Data Processing. NMR spectra were obtained on a Varian Unity*plus* 750 MHz NMR spectrometer equipped with four RF channels, a Performa II *z* axis pulsed field gradient (PFG) accessory, and a Varian $^{1}H/^{13}C/^{31}P/^{2}H$ four-channel probe with a PFG coil. Unless otherwise noted, all experiments were performed at 25.0 ± 0.1 °C. The solvent signals were used as internal references for both ^{1}H and ^{13}C chemical shifts. In the $CDCl_3$/$CHCl_3$ solution, the chemical shifts were referenced relative to the $CHCl_3$: ^{1}H chemical shift at 7.27 ppm and ^{13}C chemical shift at 77.23 ppm. In the C_6D_6/C_6H_6 solution, the chemical shifts were referenced relative to the C_6H_6: ^{1}H chemical shift at 7.16 ppm and ^{13}C chemical shift at 128.39 ppm. All data were processed with Varian's VNMR software on a SUN Ultra-10 workstation.

NMR Measurement. (a) 1D NMR Experiments. The ^{1}H spectra of all dendrimers were acquired at 750 MHz by using a 3.5 s acquisition time, 8 kHz spectral width, 3.1 μs (30°) pulse width, and 16 transients. All ^{13}C spectra were acquired at 188.6 MHz by using a 1.0 s acquisition time, 20 kHz spectral width, 4.6 μs (45°) pulse width, and 64 transients with WALTZ-16 modulated ^{1}H decoupling.

(b) 2D NMR Experiments. The HMQC-TOCSY 2D-NMR[28] spectrum of DAB-16 was collected with ^{1}H and ^{13}C 90° pulses of 8.4

(18) Bosman, A. W.; Bruining, M. J.; Kooijman, H.; Spek, A. L.; Janssen, R. A. J.; Meijer, E. W. *J. Am. Chem. Soc.* **1998**, *120*, 8547.

(19) (a) Meltzer, A. D.; Tirell, D. A.; Jones, A. A.; Inglefield, P. T.; Hedstrand, D. M.; Tomalia, D. A. *Macromolecules* **1992**, *25*, 4541. (b) Meltzer, A. D.; Tirell, D. A.; Jones, A. A.; Inglefield, P. T. *Macromolecules* **1992**, *25*, 4549.

(20) Malyarenko, D. I.; Vold, R. L.; Hoatson, G. L *Macromolecules* **2000**, *33*, 1268.

(21) Malyarenko, D. I.; Vold, R. L.; Hoatson, G. L *Macromolecules* **2000**, *33*, 7508.

(22) Lambert, B.; Basso, E.; Qing, N.; Lim, S. H.; Pflug, J. L. *J. Organomet. Chem.* **1998**, *554* (2), 113.

(23) Chai, M.; Pi, Z.; Tessier, C.; Rinaldi, P. L. *J. Am. Chem. Soc.* **1999**, *121*, 273.

(24) Chai, M.; Niu, Y.; Youngs, W. J.; Rinaldi, P. L. *Macromolecules*. In press.

(25) (a) Wijmenga, S. S.; Hallenga, K.; Hilberts, C. W. *J. Magn. Reson.* **1989**, *84*, 634. (b) Spitzer, T. D.; Martin, G. E.; Crouch, R. C.; Shockcor, J. P.; Farmer, B. T., II *J. Magn. Reson*. **1992**, *99*, 433.

(26) Jeener, J.; Meier, B. H.; Bachmann, P.; Ernst, R. R. *J. Chem. Phys.* **1979**, *71*, 4546.

(27) (a) Talluri, S.; Wagner, G. *J. Magn. Reson., Ser. B* **1996**, *112*, 200. (b) Jahnke, W.; Baur, M.; Gemmecker, G.; Kessler, H. *J. Magn. Reson. Ser. B* **1995**, *106*, 86. (c) Ikura, M.; Kay, L. E.; Tschudin, R.; Bax, A. *J. Magn. Reson.* **1990**, *86*, 204.

and 18.0 μs, respectively, a relaxation delay of 1 s, $\Delta = (2 \times {}^1J_{HC})^{-1} = 3.57$ ms (optimized for 1-bond $^1H-^{13}C$ correlations), 20000 and 2000 Hz spectral windows in the $^{13}C(f_1)$ and $^1H(f_2)$ chemical shift dimensions, respectively, a 0.05 s acquisition time using ^{13}C GARP decoupling with a field strength of 4.93 kHz, and a 50 ms TOCSY isotropic mixing pulse using MLEV-16 modulation, with a field strength of 11.25 kHz after a 2.0 ms trim pulse; 16 transients were averaged for each of 2 × 1024 complex t_1 increments. The data were processed with a combination of shifted sinebell and Guassian weighting in both dimensions; linear prediction was used to forward extend the data in the f_1 and f_2 dimensions to double the original size (64 complex points were used to calculate 9 coefficients for each dimension); and zero filling was used so that 2D FT was performed on a 1024 × 8192 matrix.

Two NOESY 2D-NMR spectra of DAB-16 were collected: one with 7981 Hz spectral windows in f_1 and f_2 and a 2 s mixing time to detect the NOE interactions between solvent protons and dendrimer protons, and a second with 2236 Hz spectral windows in f_1 and f_2 and a 0.75 s mixing time to detect the NOE interactions among dendrimer protons. ^1H 90° pulses were between 8.6 and 11.3. All the NOESY 2D experiments were performed with a 1.5 s relaxation delay and a 0.256 s acquisition time; 16 transients were averaged for each of 2 × 512 complex t_1 increments. The data were processed with Gaussian weighting in both dimensions and zero filling to a 2048 × 4096 data matrix before Fourier transformation.

(c) 3D NMR Experiments. The HMQC-TOCSY 3D-NMR spectrum of DAB-16 was collected with ^1H and ^{13}C 90° pulses of 8.8 and 18.0 μs, respectively, a relaxation delay of 1 s, $\Delta = (2 \times {}^1J_{HC})^{-1} = 3.57$ ms (optimized for 1-bond $^1H-^{13}C$ correlations), 3405.1, 1799.9, and 1799.9 Hz spectral windows in the $^{13}C(f_1)$, $^1H(f_2)$, and $^1H(f_3)$ chemical shift dimensions, respectively, a 0.05 s acquisition time using ^{13}C GARP decoupling with a field strength of 19.7 kHz, and a 50 ms isotropic mixing time using the MLEV-17 sequence with a field strength of 11.25 kHz after a 2.0 ms trim pulse; 4 transients were averaged for each of 2 × 56 complex t_1 increments and 2 × 56 complex t_2 increments. Homospoil gradient pulses were used to purge undesired transverse magnetization. The data were processed with a combination of shifted sinebell and Gaussian weighting in all three dimensions; linear prediction was used to forward extend the data in the f_1, f_2, and f_3 dimensions to increase the digital resolution (64 complex points were used to calculate the f_3 coefficients, 48 complex points were used to calculate f_1 *and* f_2 coefficients); and zero filling was used so that 3D FT was performed on a 1024 × 512 × 512 3D matrix. To enhance the resolution of the 3D spectrum, to reduce the data size, and to reduce the experiment time, a very narrow ^{13}C spectral window (~3 kHz) was used. Consequently some peaks are aliased into regions where they do not interfere with other resonances in the spectrum. The ^{13}C chemical shifts of the 3D spectrum were traced back to those of the 1D spectrum.

The NOESY-HSQC 3D-NMR spectrum of DAB-16 was collected with ^1H and ^{13}C 90° pulses of 9.4 and 18.0 μs, respectively, a relaxation delay of 1 s, $\Delta = (2 \times {}^1J_{HC})^{-1} = 3.57$ ms (optimized for 1-bond $^1H-^{13}C$ correlations), a mixing time of 0.5 s, 1800, 7500.5, and 1800 Hz spectral windows in the $^1H(f_1)$, $^{13}C(f_2)$, and $^1H(f_3)$ chemical shift dimensions, respectively, and a 0.05 s acquisition time using ^{13}C GARP decoupling with a field strength of 19.7 kHz; 16 transients were averaged for each of the 2 × 48 complex t_1 increments and the 2 × 48 complex t_2 increments. Pulsed field gradients were used to purge undesired transverse magnetization and to compensate imperfect 180° pulses. The data were processed with a combination of shifted sinebell and Gaussian weighting in all three dimensions, and zero filling was used so that 3D FT was performed on a 512 × 1024 × 512 3D matrix.

Results and Discussion

Because the DAB dendrimers have been synthesized by the divergent method, defects exist in the higher generation dendrimers. Dendrimers having generations 1−4 have been examined by 750 MHz NMR. Defects were evident from the NMR spectra of DAB-32 (generation 4); no obvious defects were evident from the NMR spectra of DAB-16 (generation 3). The structure of DAB-16 provides the complexity needed to represent the overall features of the DAB dendrimer system,

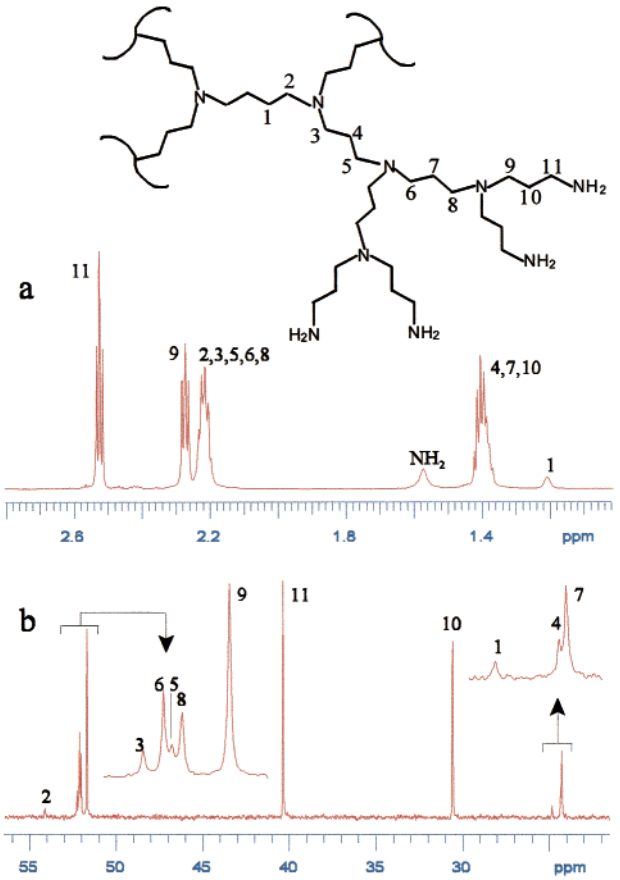

Figure 1. 1D NMR spectra of 0.16 M DAB-16 in chloroform: (a) ^1H NMR spectrum at 750 MHz and (b) ^{13}C NMR spectrum at 188.6 MHz.

and it is simple enough to resolve all the resonances and interpret the spectra by simple inspection of the 2D and 3D NMR spectra. Consequently, DAB-16 was used as the basis for the first NMR studies reported here.

NMR Characterization. There are eleven unique methylene groups in DAB-16, which are numbered from the core to the exterior of the dendrimer (see Figure 1). The exponential growth of dendritic chains produces a much larger number of methylenes (9−11) at the exterior than at the core; these contribute to very strong signals in the NMR spectra. The resonances from the interior methylenes (3−8) of DAB-16 produce strongly overlapping multiplets due to their very similar surroundings. The resonances from core methylenes (1 and 2) are dramatically weaker because of their very low occurrences in the structure. The 750 MHz ^1H NMR spectrum (Figure 1a) exhibits four intense multiplets near 2.53, 2.28, 2.22, and 1.39 ppm, as well as two small broad peaks at ~1.57 and ~1.21 ppm. The broad signal near 1.57 ppm is from the exchangeable $-NH_2$ protons. The others are from various methylene protons of DAB-16. The two triplets near 2.53 and 2.28 ppm can be assigned to the protons of methylene groups 11and 9, respectively. The resonances from the $-NCH_2-$ type methylenes of the interior overlap with the multiplets near 2.22 ppm. The remaining upfield multiplets are attributed to methylene groups 4, 7, and 10. The tiny broad peak at 1.21 ppm is assigned to methylene 1 of the core. The signal from methylene 2 is buried under the multiplets near 2.22 ppm. Further detailed assignments for the proton resonances cannot be obtained by simple inspection of the 1D ^1H NMR spectrum. Fortunately, the 188.6 MHz ^{13}C NMR spectrum (Figure 1b) exhibits eleven resolved resonances for DAB-16. On the basis of their relative intensities, we can

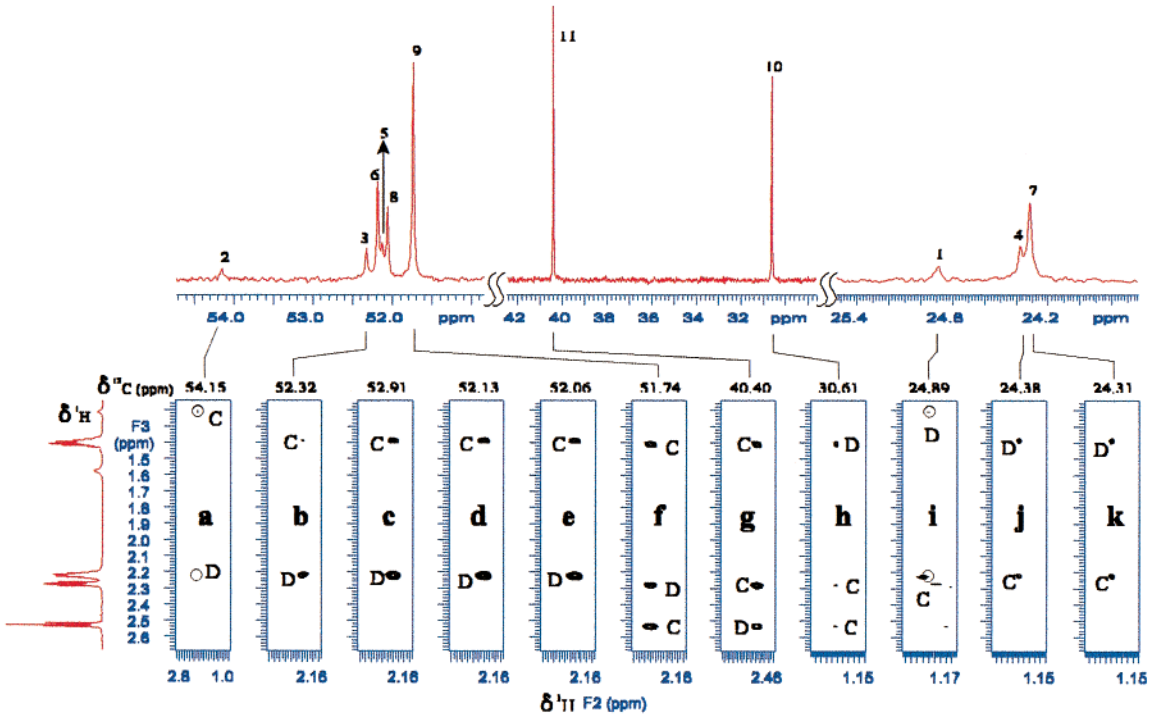

Figure 2. Eleven f_2f_3 slices (**a**−**k**) from the 3D HMQC-TOCSY spectrum of 0.16 M DAB-16 in chloroform with the 1D ^{13}C and ^{1}H NMR spectra displayed along the top and the side, respectively. The resonance assignments are labeled on the 1D ^{13}C NMR spectrum. The ^{13}C chemical shift (f_1) is labeled above each slice, the peaks marked D are the diagonal peaks, and the peaks marked C are the TOCSY cross-peaks.

assign the smallest peaks at 24.89 and 54.15 ppm to C_1 and C_2 of the core, respectively. The very intense peaks at 51.74 and 40.40 ppm are attributed to the carbons of the exterior $-NCH_2-$ groups (C_9 and C_{11}). The remaining strong signal at 30.61 ppm is from C_{10}. In the downfield region of the spectrum, four very closely spaced resonances at 52.32, 52.19, 52.13, and 52.06 ppm are from the carbons of the interior $-NCH_2-$ type methylenes (C_3, C_5, C_6, and C_8). On the basis of the intensities of these signals, the relatively weak peaks at 52.32 and 52.13 ppm are most likely from C_3 and C_5, and the relatively strong peaks at 52.19 and 52.06 ppm are most likely from C_6 and C_8. In the upfield region, there are two closely spaced peaks at 24.38 and 24.31 ppm, which can be assigned to C_4 and C_7, respectively. On the basis of the well-resolved carbon resonances, complete ^{1}H NMR resonance assignments of DAB-16 have been obtained by 3D ^{13}C edited HMQC-TOCSY NMR experiment.[28]

Figure 2 shows f_2f_3 slices from the 3D HMQC-TOCSY spectrum at the shifts of each ^{13}C resonance in the f_1 dimension. Each 2D slice contains two or three peaks, one corresponding to the diagonal peak (D) and one or two to cross-peaks (C). Figure 2a and 2i display the TOCSY correlations among the core methylene protons of DAB-16. Only two types of methylene protons are present in the core of the dendrimer, producing unique slices with only two TOCSY correlations. It is straightforward to assign the proton resonance at 2.24 ppm to the H_2 ($-NCH_2-$) of the core and the proton resonance at 1.21 ppm to H_1 ($-CH_2-$) of the core, based on the relative ^{1}H shifts. Similarly, resonances shown in the remaining slices can be attributed to the interior and exterior methylene protons of the dendrimer. Figures 2b−e and 2j,k all contain two strong peaks at 2.22 and 1.39 ppm. Considering that all methylene protons of the interior are located in nearly identical environments, all interior $-NCH_2-CH_2-CH_2N-$ units are chemically very similar. Thus only two types of proton resonances are resolved in each of these slices, at 2.22 ppm from the $-NCH_2-$ groups and at 1.39 ppm from the $-CH_2CH_2CH_2-$. The exterior propylene units of DAB-16 are bound to primary and tertiary amine groups which differentiate them. Therefore, three peaks are expected in the TOCSY slices at the shifts of C_9, C_{10}, and C_{11}, one diagonal peak and two cross-peaks. Figures 2f−h show the TOCSY slices extracted from the 3D HMQC-TOCSY spectrum at the ^{13}C chemical shifts of each exterior methylene carbon. The signal at 2.53 ppm is from H_{11}. The peak at 2.28 ppm is attributed to H_9 and the peak at 1.41 ppm is attributed to H_{10}. In this way we can resolve and assign all proton resonances in the 3D spectrum. The ^{13}C and ^{1}H chemical shift assignments are summarized in Table 2.

In benzene solution, both the ^{1}H and the ^{13}C resonances are better dispersed in the 1D-NMR spectra (see Supporting Information) compared to the corresponding spectra in chloroform. One consequence of this improved dispersion in the 1D NMR spectra is that the resonance assignments of DAB-16 in benzene can be accomplished by using a 2D HMQC-TOCSY experiment. Figure 3 shows the 2D HMQC-TOCSY spectrum of DAB-16. This spectrum provides information similar to that found in the 3D HMQC-TOCSY. In the same way, this spectrum provides the complete assignments of ^{1}H and ^{13}C chemical shifts, which are marked on the spectrum in Figure 3 and are summarized in Table 2. The NH_2 protons in the ^{1}H 1D-NMR spectrum are buried under the H_{10} resonance; this is evident from the integration values. Because there is no coupling between the NH_2 protons and the rest of the atoms in the molecule, these protons cannot be observed in the HMQC-TOCSY 2D-NMR spectrum. NOE studies described below

(28) (a) Bax, A.; Lerner, L. *J. Magn. Reson.* **1986**, *69*, 375−380. (b) Domke, T. *J. Magn. Reson.* **1991**, *95*, 174−177. (c) John, B. K.; Plant, D.; Heald, S. L.; Hurd, R. E. *J. Magn. Reson.* **1991**, *94*, 664. (d) Willker, W.; Leibfritz, D.; Kerssebaum, R.; Bermel, W. *Magn. Reson. Chem.* **1993**, *31*, 287−292.

(29) Neuhaus, D.; Williamson, M. P. *The Nuclear Overhauser Effect in Structural and Conformational Analysis*; VCH Publishers: New York, 1989.

(30) Noggle, J. H.; Schirmer, R. E. *The Nuclear Overhauser Effect in Chemical Applications*; Academic Press: New York, 1971; p 59.

Table 2. ^{13}C and ^{1}H Chemical Shift Assignments for DAB-16

	chemical shifts (ppm)			
	$\delta^{13}C$ (ppm)		$\delta^{1}H$ (ppm)	
methylene no.	chloroform	benzene	chloroform	benzene
1	24.89	26.14	1.21	1.56
2	54.15	55.20	2.24	2.51
3	52.32	53.36	2.22	2.52
4	24.38	25.93	1.39	1.69
5	52.13	53.25	2.22	2.50
6	52.19	53.21	2.22	2.48
7	24.31	25.86	1.39	1.64
8	52.06	53.21	2.22	2.44
9	51.47	52.76	2.28	2.42
10	30.61	32.01	1.41	1.53
11	40.40	41.39	2.53	2.66
NH_2			1.57	1.52

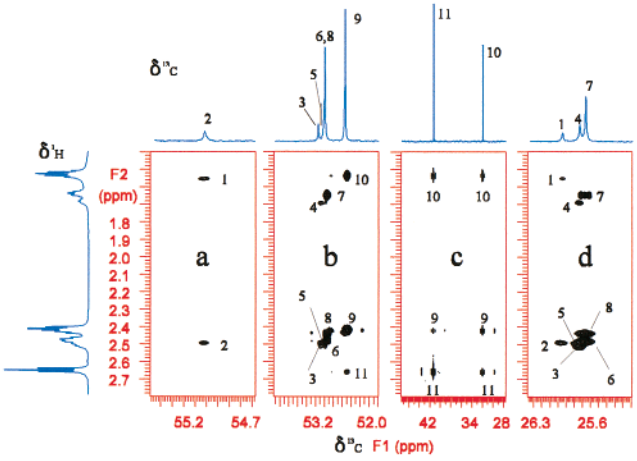

Figure 3. Expansions from the 2D HMQC-TOCSY NMR spectrum of 0.32 M DAB-16 dendrimer in benzene with 1D ^{1}H and ^{13}C NMR spectra plotted on the side and at the top, respectively.

showed that these protons are correlated with the remaining protons in the molecule. In this way the NH_2 proton resonance assignments can be confirmed. Additionally, the NH_2 proton chemical shifts in solutions vary with concentration because they are exchangeable. Thus unambiguous NMR resonance assignments can be established from this 2D-NMR experiment and the supporting studies described below.

It is interesting to compare the proton chemical shifts of DAB-16 in benzene with those in chloroform (Table 2). The chemical shifts of protons are well dispersed in benzene as mentioned above. However, the dispersion is greatly diminished in chloroform, especially for the interior protons of dendritic chains. This could be partly due to the absence of hydrogen bonding between the solvent and components of the dendrimer interior, thereby partially excluding benzene from the interior of the dendrimer to create solvent-rich and solvent-poor environments for the outer and inner parts of the dendrimer, respectively. While benzene does impart bulk susceptibility influences on chemical shifts due to its unique ring current effects, the differential proton chemical shift behavior is consistent with specific and differential solvent interactions. For example, H_4, H_7, and H_{10} (with nearly identical environments with respect to the covalent bonding network) have nearly identical shifts of 1.39, 1.39, and 1.41 in $CHCl_3$. These same protons have chemical shifts of 1.69, 1.64, and 1.53 in benzene. This solvent-induced differential chemical shift could be a consequence of direct interactions with benzene or an indirect effect such as a solvent-induced change in conformation. However, the progressive upfield shift proceeding from the interior to exterior of the dendrimer, in benzene solvent, is consistent with a progressively greater interaction with benzene ring currents as protons approach a solvent-rich dendrimer surface.

These relative shift differences are consistent with a model involving different interactions between the dendrimer and the two solvents. Unlike chloroform, benzene is nonpolar and aprotic, and the strong interactions between a proton-donor solvent, such as chloroform, and the dendrimer core are not possible with benzene. Consequently in benzene solution, the solvent molecules might prefer to reside outside the dendrimer molecules, and in chloroform, the solvent molecules might significantly permeate the interior of the dendrimer. Therefore the resonances of each of the interior protons of DAB-16 in benzene are resolvable because of the differences in their solvent environments. In chloroform, the corresponding resonances are not resolvable. If chloroform can migrate into the core of the DAB-16, this interaction will be stabilized by hydrogen bonding between the acidic chloroform protons and the interior amine groups. Thus methylene groups 3, 5, 6, 8, and 9 are expected to see similar environments through their covalent bonding network, and they also are expected to see similar environments when noncovalent interactions with neighboring structures are considered. Benzene can participate as a hydrogen bond acceptor; since only the surface nitrogens contain protons, this would tend to favor benzene−dendrimer interactions at the outer surface of the dendrimer rather than at the interior nitrogens.

Studies of Solvent Interactions with the Dendritic Chain. In the 1D NMR spectra of DAB-16 in chloroform, the resonances were consistently shifted upfield in both ^{13}C ($\Delta\delta_{^{13}C} \sim 1.0-1.1$ ppm) and ^{1}H ($\Delta\delta_{^{1}H} \sim 0.5$ ppm) spectra when the concentration was increased from 0.1 to 0.4 M. However, similar spectra of benzene solutions showed very little influence of concentration on the chemical shifts ($\Delta\delta_{^{13}C} \sim 0.25$ ppm and $\Delta\delta_{^{1}H} \sim 0.1$ ppm) (see Supporting Information). This further supports the model for the interaction between solvent and dendrimer molecules described above. Because of these interactions, the dendritic chain might populate extended conformations to a higher degree in chloroform solvent. However, in benzene, which is less likely to permeate the core of the DAB molecules, the dendrimer arms might tend to fold back into the dendrimer.

Two-dimensional NOESY NMR experiments were used to study solvent interactions with DAB dendrimers for both polar (chloroform) and nonpolar (benzene) solvents. For this purpose, mixtures of protonated and deuterated solvents were used to satisfy the simultaneous requirements for a deuterium lock signal and protons to produce a solvent−dendrimer NOE. Relatively long mixing times were used to provide time for the buildup of cross-peaks from intermolecular NOE's (which are governed be the specific intermolecular $^{1}H-^{1}H$ dipole−dipole T_1 relaxation times). One might ordinarily be concerned that significant spin diffusion would occur during such long mixing times, resulting in NOE cross-peaks between nonadjacent protons. However, if spin diffusion did occur, NOE cross-peaks would be expected among all the dendrimer resonances. The observed NOE cross-peaks in both $CHCl_3$ (Figure 4a) and benzene (Figure 4b) are quite specific, and are not consistent with significant spin diffusion. In chloroform solution, clear NOE cross-peaks between solvent protons and the dendritic chain (except the core) were observed in the 2D NOESY spectrum (Figure 4a), while in benzene solution, no such cross-peaks were observed (Figure 4b). These data support the model described above in which chloroform molecules can penetrate into the DAB dendrimer

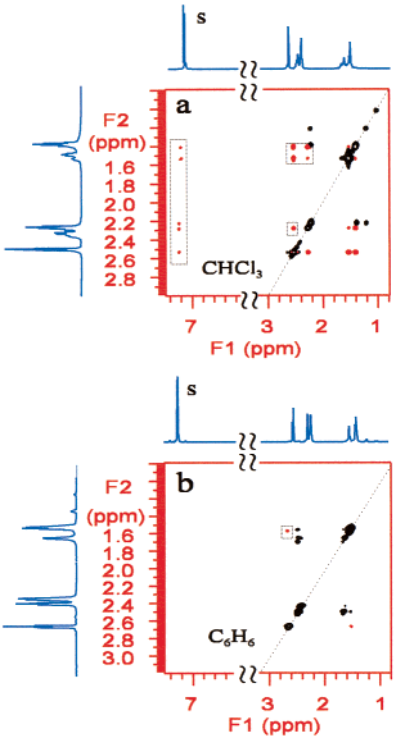

Figure 4. Selected regions from the 2D NOESY NMR spectra of the DAB-16 dendrimer obtained with 2 s mixing times and large spectral windows which include solvent peaks: (a) 0.12 M in chloroform (4:1 $CHCl_3/CDCl_3$) and (b) 0.32 M in benzene (3:1 C_6H_6/C_6D_6); here solvent peaks in both 1D plots are marked with S. (The positive NOE cross-peaks are framed within rectangles on one side of the diagonal.)

to "solvate" the dendritic chain, while benzene molecules are less likely to penetrate the interior of the DAB molecules.

Conformational Studies of Dendritic Chains in Solutions. Proton−proton NOE interactions can also supply information about the spatial relationships among protons of the dendritic chains, which are related to their conformations. If benzene is significantly excluded from the interior of the DAB dendrimer, folded chain conformations might be expected to fill voids in the interior of the dendrimer in benzene solutions. However, in chloroform solutions, the chain conformations are expected to be predominantly extended to permit the solvent permeation to the interior of the dendrimer. In the former case, more NOE interactions among dendritic chain protons are expected in folded chain conformations because of the closer proximity of these protons, while fewer NOE interactions among dendritic chain protons are expected in extended chain conformations. To focus on the dendritic chain NOE interactions, NOESY spectra with narrow spectral windows to include only peaks from dendritic chains were collected. In this way, spectra with extremely good digital resolution were obtained.

Figure 5 shows NOESY spectra of DAB-16 in chloroform (Figure 5a) and in benzene (Figure 5b). In all these figures, both positive and negative NOE cross-peaks are observed, consistent with local motion on both the short ($\omega^2\tau_c^2 < 1$) and the long ($\omega^2\tau_c^2 > 1$) sides of the extreme narrowing limit, respectively, where ω is the spectrometer frequency and τ_c is the correlation time for molecular motion.[29] These observations are consistent with the expectation that the molecular segments in the core of the dendrimer have restricted motion compared to the surface segments. The molecular weight of DAB-16 (ca. 1800) approaches the range of several thousand where the T_1 minimum exists for most molecules at very high magnetic field.

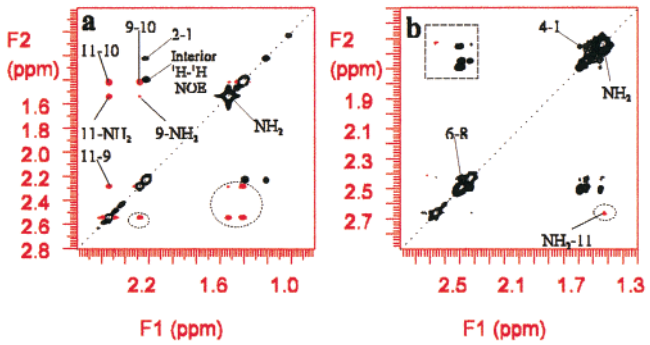

Figure 5. 2D NOESY NMR spectra of the DAB-16 dendrimer obtained with the 0.75 s mixing times and narrow spectral windows: (a) 0.12 M in chloroform and (b) 0.12 M in benzene. (The positive NOE cross-peaks are enclosed within ovals on one side of the diagonal.)

Intermolecular hydrogen bonding at the dendrimer surfaces, combined with the reduced motion of the highly branched core of DAB-16, further restricts motion; therefore, it is not surprising that motion in this part of the molecule is in the regime where $\omega^2\tau_c^2 > 1$. The protons on the surface of the dendrimer, or the exterior protons, have additional motional degrees of freedom and can tumble faster than the protons located inside the dendrimer. Thus it is possible to have both positive and negative NOE's among protons in the same molecule.

To discount the possibility of the negative NOE's arising from the "three spin effect"[30] or some other unusual relaxation phenomenon, ^{13}C T_1 experiments were performed under a variety of conditions. The ^{13}C T_1 relaxation for aliphatic carbons in DAB-16 is almost entirely due to dipole−dipole interactions with directly bound protons. This makes it straightforward to relate ^{13}C T_1 values to molecular motion and τ_c. The correlation time of the dendrimer will increase with increasing concentration or decreasing temperature. The ^{13}C T_1 relaxation times of DAB-16 have been measured at different concentrations and temperatures (see Table 3) to characterize the motions of the different parts of dendrimers. Examination of the relaxation values reveals the ^{13}C T_1 relaxation times of exterior carbons (9,10, and 11) are much longer than those of the interior (3−8) and core (1 and 2) carbons, as expected considering that the exterior part of the dendrimer has more motional degrees of freedom than the interior and core. Because mobility of the dendrimer exterior is on the short τ_c side of the T_1 minimum, T_1 values of carbons 9, 10, and 11 increase with increasing temperature or with decreasing concentration. The τ_c for the core and interior carbons is at or below the value corresponding to the minimum in the plot of ^{13}C T_1 vs τ_c. Their ^{13}C T_1 values are nearly unchanged and in some cases actually decrease upon increasing the temperature. This is consistent with the interior protons showing a negative NOE (slow motion regime) and the exterior protons showing a positive NOE (fast motion regime). In concentrated chloroform (0.4 M) solution, motion is further restricted due to increased solution viscosity and increased intermolecular hydrogen bonding. As the temperature of this solution was elevated, the T_1 values of exterior ^{13}C nuclei increased noticeably, the ^{13}C T_1 values of the interior carbons were essentially unchanged, and the ^{13}C T_1 values of the core carbons diminished. These results confirm the hypothesis that the dendrimer core is in the slow motion regime (negative NOE values expected), the interior is near the crossover between the fast and slow motion regimes, and the exterior is in the fast motion regime (positive NOE values expected).

When the concentrations are increased, the ^{13}C T_1 values of both core and interior carbons increased, and the ^{13}C T_1 values

Table 3. ^{13}C T_1 Values of DAB-16 at Different Concentrations and Temperatures[a]

	T_1 in chloroform (s)				T_1 in benzene (s)			
	0.12 M		0.40 M		0.12 M		0.40 M	
methylene no.	at 25 °C	at 45 °C	at 25 °C	at 45 °C	at 25 °C	at 45 °C	at 25 °C	at 45 °C
1	0.30	0.30	0.34	0.31	0.25	0.32	0.33	0.30
2	0.26	0.26	0.32	0.27	0.24	0.27	0.33	0.26
3	0.25	0.27	0.29	0.26	0.25	0.30	0.29	0.26
4	0.29	0.33	0.30	0.30	0.26	0.32	0.31	0.31
5	0.26	0.28	0.28	0.29	0.24	0.29	0.28	0.29
6	0.26	0.37	0.28	0.29	0.30	0.38	0.28	0.29
7	0.29	0.33	0.30	0.29	0.31	0.40	0.31	0.31
8	0.26	0.28	0.28	0.26	0.30	0.38	0.28	0.29
9	0.35	0.47	0.30	0.36	0.42	0.60	0.31	0.42
10	0.53	0.76	0.43	0.56	0.67	1.00	0.46	0.68
11	0.82	1.23	0.63	0.91	1.09	1.74	0.70	1.21

[a] The relative errors for all ^{13}C T_1 values are less than ±4%.

of exterior carbons were reduced. Again, this is consistent with the core and interior protons existing in the motional regime to produce negative NOE values, and the exterior protons existing in the motional regime to produce positive NOE values. In benzene solutions, similar trends are observed, and similar conclusions can be made.

NOE studies can also contribute to the proof of the resonance assignments for DAB dendrimers. Figure 5a is the 2D NOESY spectrum of DAB-16 in chloroform. According to the chemical shift assignment, the NOE cross-peaks among core protons and among exterior protons can be clearly assigned, but the NOE cross-peaks from interior protons are heavily overlapped and their assignments cannot be completely determined. It is necessary to use a 3D NOESY-HSQC spectrum to resolve these resonances (see below) and to identify NOE interactions among interior protons based on the resolved ^{13}C chemical shifts. However, better resolution was obtained in the NOESY spectra of DAB-16 in benzene solution (Figure 5b). The NOE interactions among the protons of the dendrimer in benzene can be identified, and are labeled on the figures. When compared with the NOESY spectrum of DAB-16 in chloroform, the NOESY spectrum of DAB-16 in benzene shows more cross-peaks. In addition to NOE interactions between protons on adjacent carbons, NOE interactions among interior protons H_5 and H_6 and exterior protons H_{10} are observed in the 2D NOESY spectrum for DAB-16 in benzene (Figure 6). This indicates that the dendritic chains fold back so that parts of the dendrimer exterior are close to parts of the interior. Detailed assignments of these cross-peaks are marked in Figure 6 along with a structure with arrows showing selected NOE interactions from a folded chain conformation.

It is important to determine whether these NOE interactions are inter- or intramolecular. 2D NOESY spectra of DAB-16 in chloroform and benzene were obtained at various concentrations (data shown in the Supporting Information). Cross-peaks between the resonances of exterior protons are evident at all concentrations. Sign changes consistent with a change in τ_c from the slow to the fast motion are seen; however, NOE values are still present even in the dilute benzene solution. These data are consistent with intramolecular NOE interactions. No evidence was found for intermolecular or intramolecular penetrations for the dendrimer arms of DAB-16 in chloroform solutions. Similar results were observed by Topp et al.[25]

Because of the severe overlap of resonances in the NOESY spectra of DAB-16 in chloroform it was not possible to resolve and identify peaks characteristic of the NOE interactions among the interior protons. To circumvent this problem, a 3D NOESY-HSQC experiment was performed to disperse the overlapped

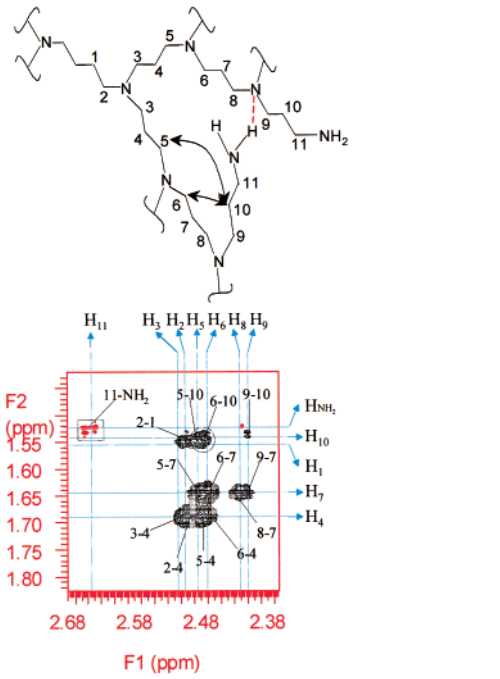

Figure 6. An expansion from the highlighted region of the 2D NOESY NMR spectrum (in Figure 5b) of 0.12 M DAB-16 in benzene with detailed resonance assignments. The positive NOE cross-peaks are framed within a rectangle. The cross-peaks within the circle in the spectrum and the positions connected by double-pointed arrows in the structure indicate the proton NOE interactions from the folded chain conformation.

NOESY cross-peaks based on the resolved ^{13}C resonances, in a manner similar to that described above for the 3D HMQC-TOCSY experiment. Selected f_1f_3 slices cut at each ^{13}C (f_2) chemical shift from the 3D NOESY-HSQC spectrum are shown in Figure 7. Figures 7a and 7i display the NOE interactions among core protons; Figures 7b−e and 7j,k show the NOE interactions among interior protons; and Figures 7f−h exhibit the NOE interactions among exterior protons. These slices only exhibit NOE interactions between protons on adjacent carbons in the dendritic chain or between similar types of protons on nearby dendritic chains. NOE interactions are not observed between protons on different segments of the chain, indicating the chain ends of the dendrimer are primarily oriented outward from the core of the dendrimer. The information obtained from this experiment is further support for a solvent−dendrimer interaction model containing primarily extended chain confor-

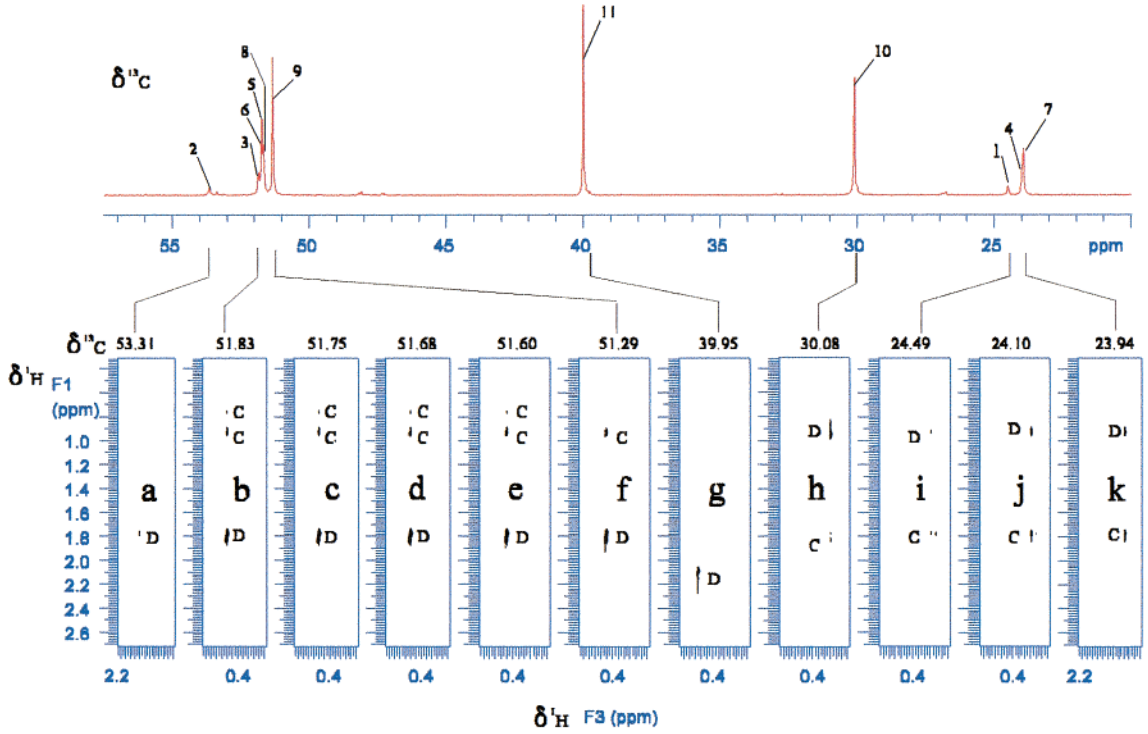

Figure 7. Eleven f_1f_3 slices (**a**−**k**) from the 3D NOESY-HSQC spectrum of 0.40 M DAB-16 in chloroform with the 1D ^{13}C NMR spectrum displayed across the top. The resonance assignments are labeled in the 1D ^{13}C NMR spectrum. The ^{13}C chemical shift (f_1) of each slice is labeled at the top; the peaks marked D are the diagonal peaks and the peaks marked C are the cross-peaks.

mations for DAB-16 in chloroform, as has been suggested by the data in the previous discussions.

Conclusion

Many computational simulations have been performed on dendrimers. However, because of the lack of sufficient experimental data, it has not been possible to determine the validity of different simulation models, especially with regard to chain conformation and density. Multidimensional NMR experiments such as 2D NOESY, 3D NOESY-HSQC, and 3D HMQC-TOCSY at very high magnetic field can be very useful for dendrimer studies. With these techniques, unambiguous chemical shift assignments of dendrimers can be obtained and information regarding chain motion and the conformation of dendrimers can be acquired. These experiments supply the experimental data needed to understand the unique structures, properties, and topologies of dendrimers. On the basis of unequivocal ^{1}H NMR resonance assignments and ^{1}H NOE interactions among the dendrimer protons, this research clearly shows that in a "good" solvent (chloroform), extended chain conformations are dominant for DAB-16, and in a "poor" solvent (benzene), folded chain conformations are observed for DAB-16, supporting computer simulation results on DAB dendrimers.[24]

Acknowledgment. We would like to acknowledge Dr. Gerhard Wagner and Dr. Gregory Heffron at Harvard Medical School for their generous help with the 3D NOESY-HSQC pulse sequence used in this work. We also would like to acknowledge the National Science Foundation (DMR-9617477 and DMR-0073346) for support of this research and the Kresge Foundation and donors to the Kresge Challenge program at the University of Akron for funds used to purchase the 750 MHz NMR instrument.

Supporting Information Available: 1D, 2D, and 3D NMR data for DAB-16 (PDF). This material is available free of charge via the Internet at http://pubs.acs.org.

JA002824M